Supplementary Information

Low operating voltage carbon-graphene hybrid e-textile for temperature sensing

Gopika Rajan[1], Joseph J. Morgan[1], Conor Murphy,[1] Elias Torres Alonso[1], Jessica Wade[2], Anna K. Ott[1], Saverio Russo[1], Helena Alves[3,4], Monica F. Craciun[1], Ana I. S. Neves[1*]

[1] College of Engineering, Mathematics and Physical Sciences, University of Exeter, North Park Road, EX4 4QF, Exeter, United Kingdom
[2] Department of Physics and Centre for Plastic Electronics, Imperial College London, London SW7 2AZ, United Kingdom
[3] Department of Physics and CICECO, University of Aveiro, 3819-130, Aveiro, Portugal
[4] Department of Physics, Instituto Superior Técnico, University of Lisbon, Av. Rovisco Pais 1, 1040-001, Lisbon, Portugal

* a.neves@exeter.ac.uk

1. Trilayer graphene (TLG) films

The purpose of developing this type of graphene was to increase the number of layers above the single-layer and below the commercially available FLG, which has an average of 4 layers, ranging from 1 to 7, described by the manufacturer as "patchwork", with patches of different thickness. Transmittance was used to estimate the number of layers in the same films, using the method described by Zhu *et al.* [1], with the following relation $T = (1+1.13\pi\alpha N/2)^{-2}$, with N being the number of graphene layers, $\alpha = e\hbar 2/c \approx 1/137$ which is fine structure constant and 1.13 is the estimation of the correction coefficient. The experimental data for optical transmittance in TLG graphene was extracted at 550 nm since it is independent of the stacking sequence [2]. Figure S1 shows the transmittance vs. wavelength plots of three samples of TLG (a, b and c), and S1d is a table with the calculated number of layers for each transmittance value taken at 550 nm.

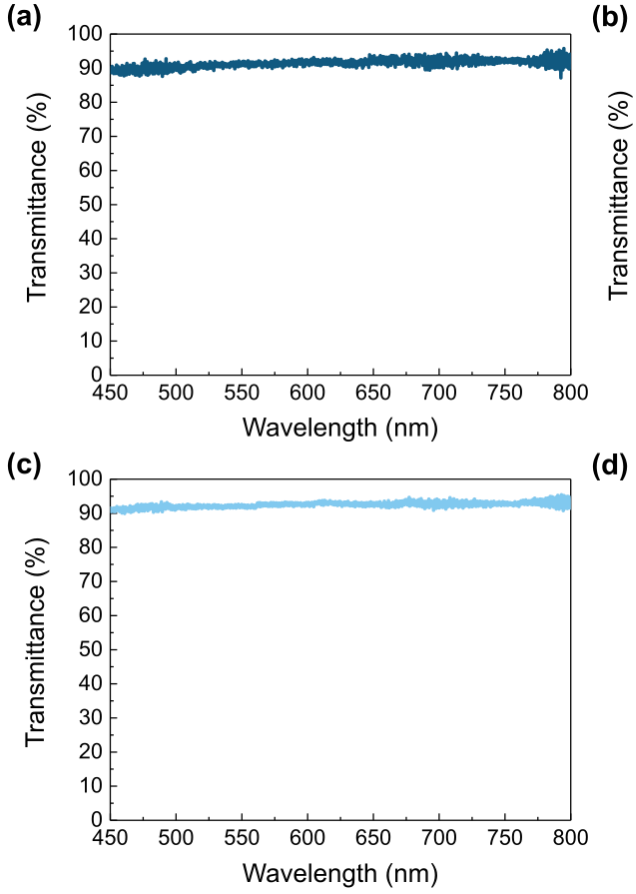

at 550 nm	Transmittance (%)	Number of layers
Sample 1	93.30	2.7
Sample 2	89.10	3.5
Sample 3	92.41	3.3

Figure S1. Transmittance of TLG on glass in: **(a)** sample 1; **(b)** sample 2; **(c)** sample 3. **(d)** Table with the number of layers calculated at the transmittance taken at 550 nm.

It has been suggested that for CVD graphene, the standard Raman spectroscopy cannot be explicitly used to quantify the number of layers; it can only be used to give an indication of the number of layers. The National Physical Laboratory (NPL) has published guidelines on the characterisation of graphene [3]. In this guide, they state that Raman spectroscopy can be used only to indicate the number of layers in a CVD graphene sample. The indicators for monolayer graphene are a FWHM {2D} < 35 cm^{-1} and a relative G and 2D band intensity of $I_{2D}/I_G > 2$. In principle, this ratio can be discrete and be used to estimate the number of layers. However, it has been found that the 2D peak depends quite strongly on carrier density and less strongly on number of layers. Therefore, since the carrier density is affected b impurities, I_{2D}/I_G is not reliable metric for the number of layers [3]. NPL states that these parameters can only be used as indicators, as both the FWHM and relative intensities can both be affected by strain and doping in the graphene. Additionally, certain bilayer graphene superlattice configurations (with specific, small mismatch angles) can fit these Raman criteria for monolayer graphene.

A more convenient approach by Koh *et al.*, also based on Raman spectroscopy, was used to estimate the number of layers of graphene on Si/SiO_2 [4]. It has been found that the ratio of intensity of G peak and the first order optical phonon peak of Si are discrete and hence can be used to find the number of layers of graphene. This is because the increase in absorption and Raman scattering of light as the number of layers increases [4]. By using the data provided by Koh *et al.* as calibration, the number of layers was found to be three with I_G/I_{Si} to be 0.2 as shown in Fig 2b. Raman mapping was performed to understand that distribution of the number of layers (figure S2).

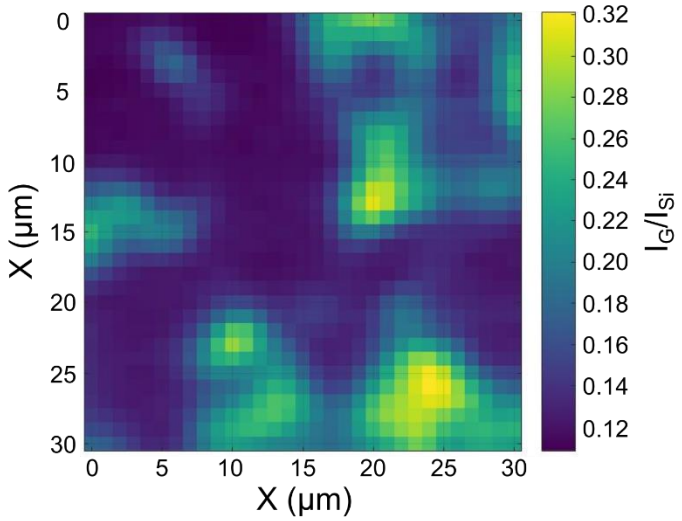

Figure S2. Raman map of 30 × 30 μm^2 of TLG on Si/SiO_2.

2. Graphene-coated PP fibres

Raman spectroscopy was used to confirm the presence of graphene coating the surface of the polypropylene (PP) fibres. Figure S3 shows the Raman spectra of (top to bottom): uncoated PP fibre; PP fibre coated with single-layer graphene (SLG); PP fibre coated with few-layer graphene (FLG); and PP fibre coated with shear-exfoliated graphene (SEG). The dashed lines indicate the positions expected for D, G and 2D peaks in SGL.

As can be seen in Figure S3a, the D peak region (ca. 1350 cm^{-1} for SLG) is relatively close to one of the PP peaks. It is very small in the case of SLG, and not distinguishable from the PP background. As for the G peak (ca. 1580 cm^{-1} for SLG), it appears to be relatively small in the case of SLG than for TLG, FLG and SEG, which is in agreement with the fact the 2D peak in this case is more intense. For TLG, FLG and SLG the 2D peak is almost indistinguishable from the PP peaks nearby, and the G peak is red-shifted, as expected for graphene samples with an increasing number of layers.

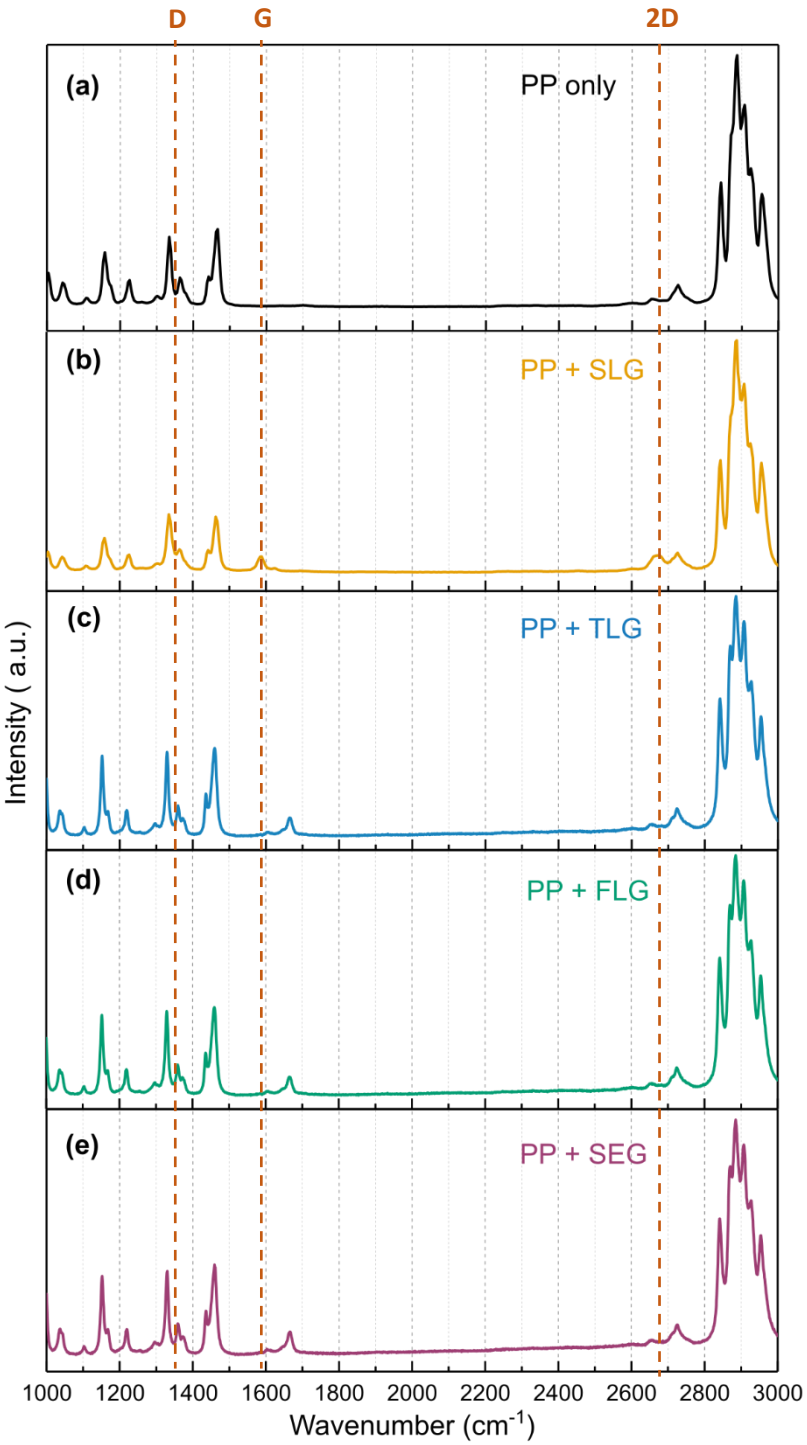

Figure S3. Raman spectra of: **(a)** uncoated PP fibre; **(b)** PP + SLG; **(c)** PP + TLG; **(d)** PP + FLG; and **(e)** PP + SEG. Dashed lines show the expected position of the D, G and 2D peaks in SLG.

3. Temperature sensing

Devices fabricated using FLG showed no visible change in resistance with temperature with either type of contact, carbon (figure S4a) and silver (figure S4b). Figures S4c and d show the same measurement for SEG coated fibres, indicating some sensitivity towards the change in temperature with both types of contacts. However, these measurements are not reproducible after a single temperature cycle (figures S4e and f). The results seem to be slightly better with carbon contacts for the case of SEG, but still not good enough for sensing applications.

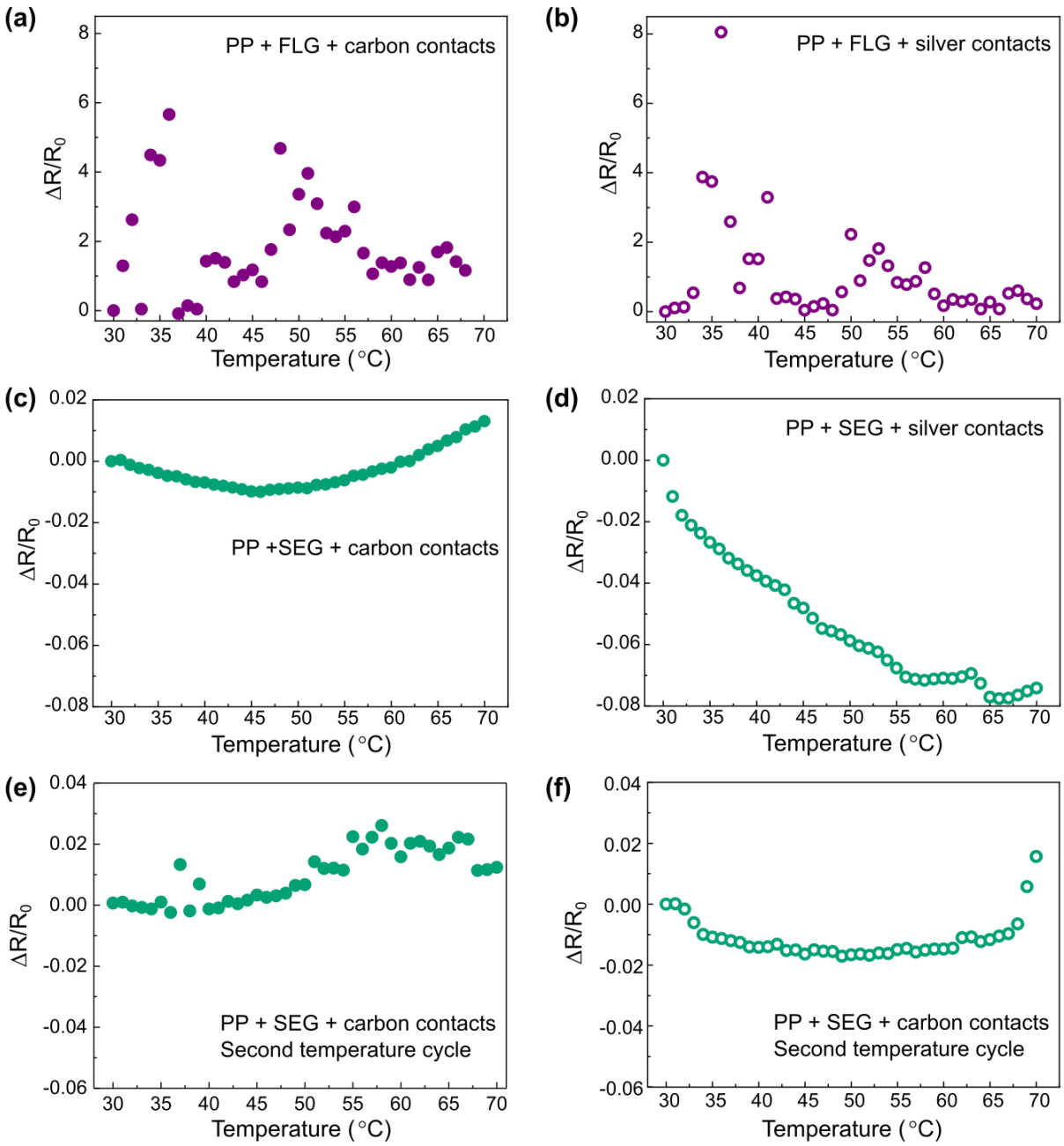

Figure S4. Sensitivity as a function of temperature for PP coated with **(a)** FLG with carbon contacts; **(b)** FLG with silver contacts; **(c)** SEG with carbon contacts; **(d)** SEG with silver contacts; second temperature cycle for PP coated with SEG with **(e)** silver contacts and **(f)** silver contacts.

Figure S5 shows the irreproducibility of SLG coated PP fibre sensors with an increasing number of temperature cycles. These cycles were only from 30 to 45°C, and still the devices that seemed to indicate a linear response to increasing temperature showed no sensing ability after only four cycles. This effect was observed in devices with carbon contacts (figure S5a) and with silver contacts (figure S5b). We believe that the graphene single layer, being thinner and not offering any redundancy like with all other types of graphene coating, is somehow damaged by temperature cycle. For this reason, SLG coatings were not further explored for sensing in this work.

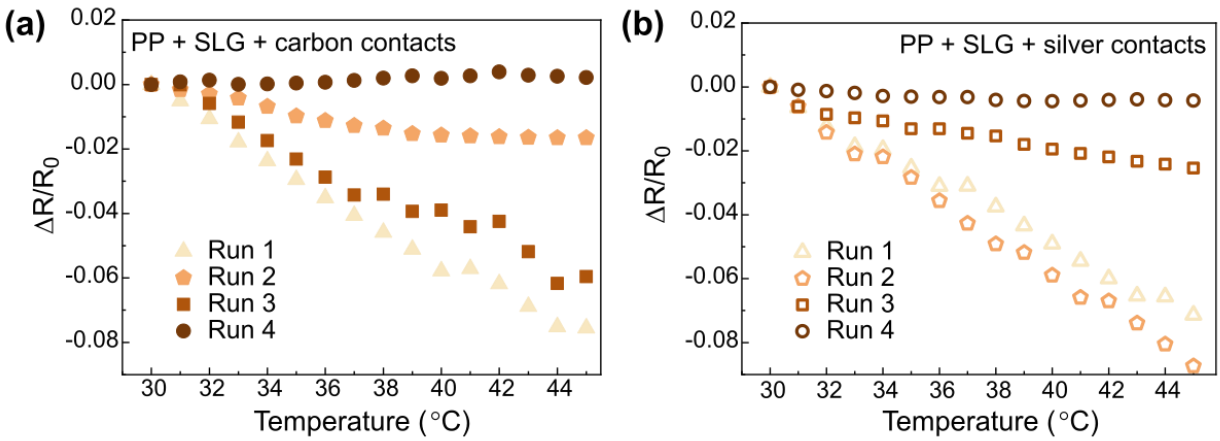

Figure S5. Sensitivity as a function of temperature for PP coated with SLG with carbon contacts **(a)** and silver contacts **(b)**, showing lack of reproducibility over multiple temperature runs.

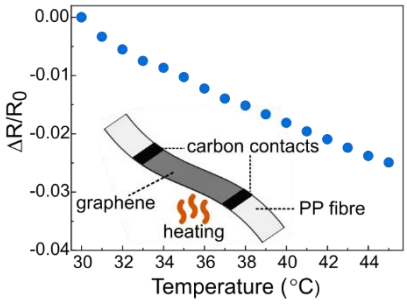

Going back to our best sensors, the ones with TLG, figure S6 shows the absolute resistance values measured for the sensor presented in figure 2a, with carbon contacts, with the error bars associated with the measurement, showing that the error is small.

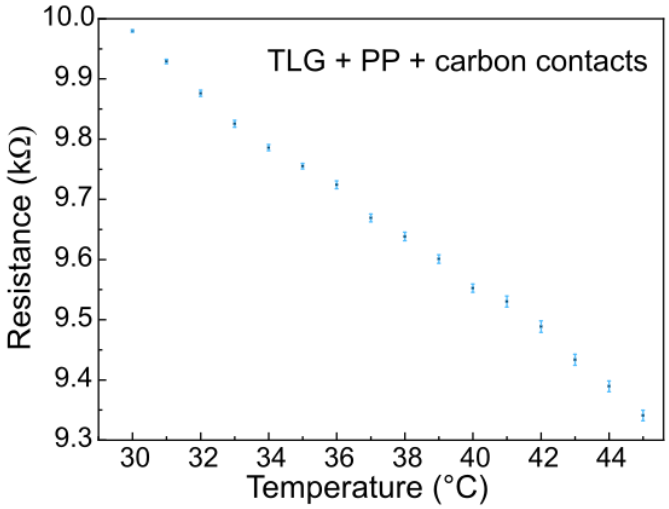

Figure S6. Resistance as a function of temperature for PP coated with TLG with carbon contacts with error bars around the human body temperature range.

An operating voltage of 0.5 V was also tested with the TLG on PP devices with carbon contacts to demonstrate the potential for even lower operating voltages. Although the response is not as good as for a 1 V, as can be

seen in figure S7, this demonstrates that, upon optimisation, the operating voltages of these sensors could be brought down even further.

The linearity of these TLG-coated PP sensors was assessed through the average linear fitting of fig. 2c (10 consecutive runs in the same sample), $y = ax + b$, is $a = 0{,}00465 \pm 0{,}000204$ and $b = 0{,}13694 \pm 0{,}006865$, indicating a reliable and robust process.

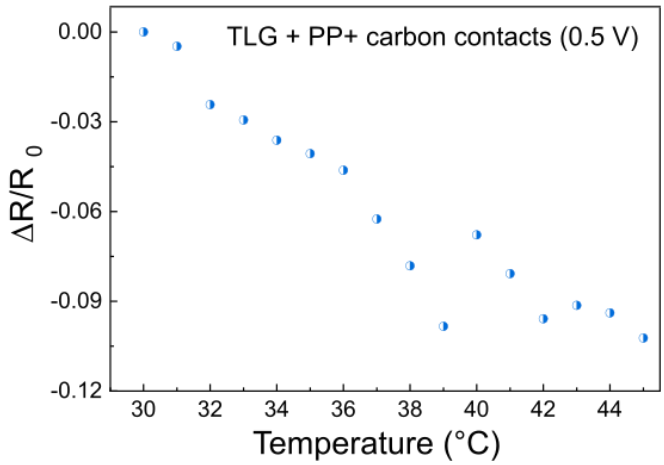

Figure S7. Resistance as a function of temperature for PP coated with TLG with carbon contacts with error bars around the human body temperature range.

We compared the performance with different types of contacts for the TLG-based sensors. Figure S7 shows similar devices, but with silver ink instead of carbon paste as contacts. Unlike the devices with carbon contacts, those with silver contacts often displayed different responses (figure S7a), and those that seemed to be sensitive to temperature in the first run proved to be unable to withstand multiple runs (figure S7b).

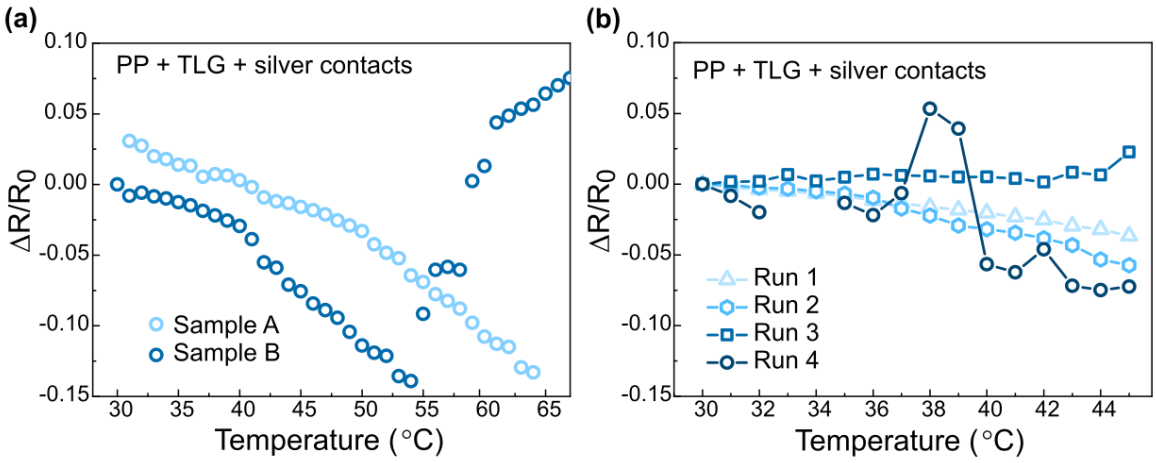

Figure S8. Sensitivity as a function of temperature for PP coated with TLG and silver contacts for: **(a)** different samples, showing irreproducibility; **(b)** for multiple runs in a sample, showing that the device is not stable.

On the other hand, the sensing behaviour of TLG devices is still observed when the measuring probes are directly connected to the graphene layer, as can be seen in figure S9, also with a linear response and

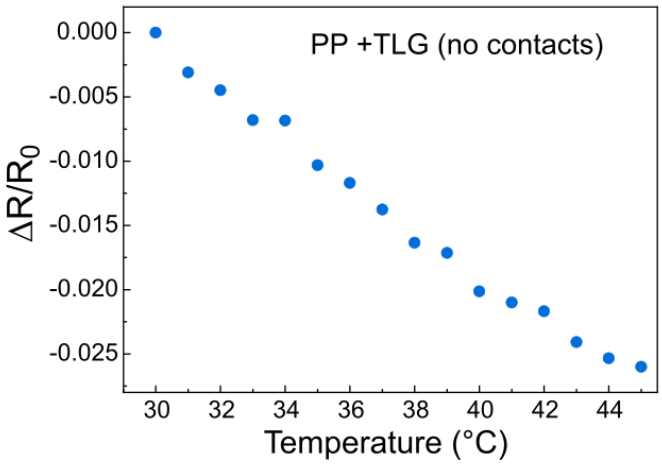

Figure S9. Sensitivity as a function of temperature for PP coated with TLG without additional contacts.

To assess the performance of these sensors in the non-contact mode, using a heat gun instead of a hot plate, to measure ambient temperature, the measurement was performed over time, against a commercial temperature sensor (Texas Instruments LM35CAZ/NOPB). This is shown in figure S10. It should be noted that here the response is shown in conductance so that the response of our sensor follows the same trend (upwards and then downwards) than the response of the commercial sensor. Our sensor's response is comparable to that of the commercial sensor as the temperature increases. However, when the heat gun was turned off (ca. 360 s, orange dashed line) our sensor seems to recover much quickly, whereas the commercial sensor displays a temperature higher than ambient temperature up to at least 1000 s.

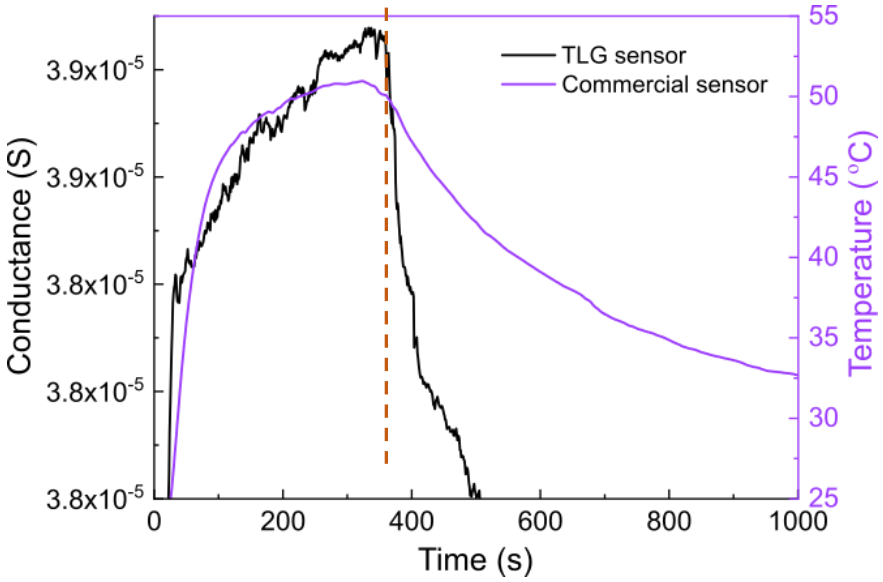

Figure S10. Ambient temperature measured over time for out TLG-based sensor and a commercial sensor.

4. Scanning Electron Microscopy (SEM)

SEM was used to investigate if the sensors suffer any morphological damage from the increase in temperature. The following images were obtained for each device before and after a room temperature to 70°C temperature cycle (figure S11). An uncoated PP fibre was subjected to the same temperature treatment, showing no discernible changes in its surface, as shown in figure S11a. We can see here the PP extrusion lines from the its production. S11b-d show that no visible damage was present in the sensors fabricated with TLG, FLG and SLG,

respectively. The CVD coatings are so thin that the extrusion lines are still visible, and we can also see some PMMA residues, inherent features of the PMMA-assisted CVD transfer process.

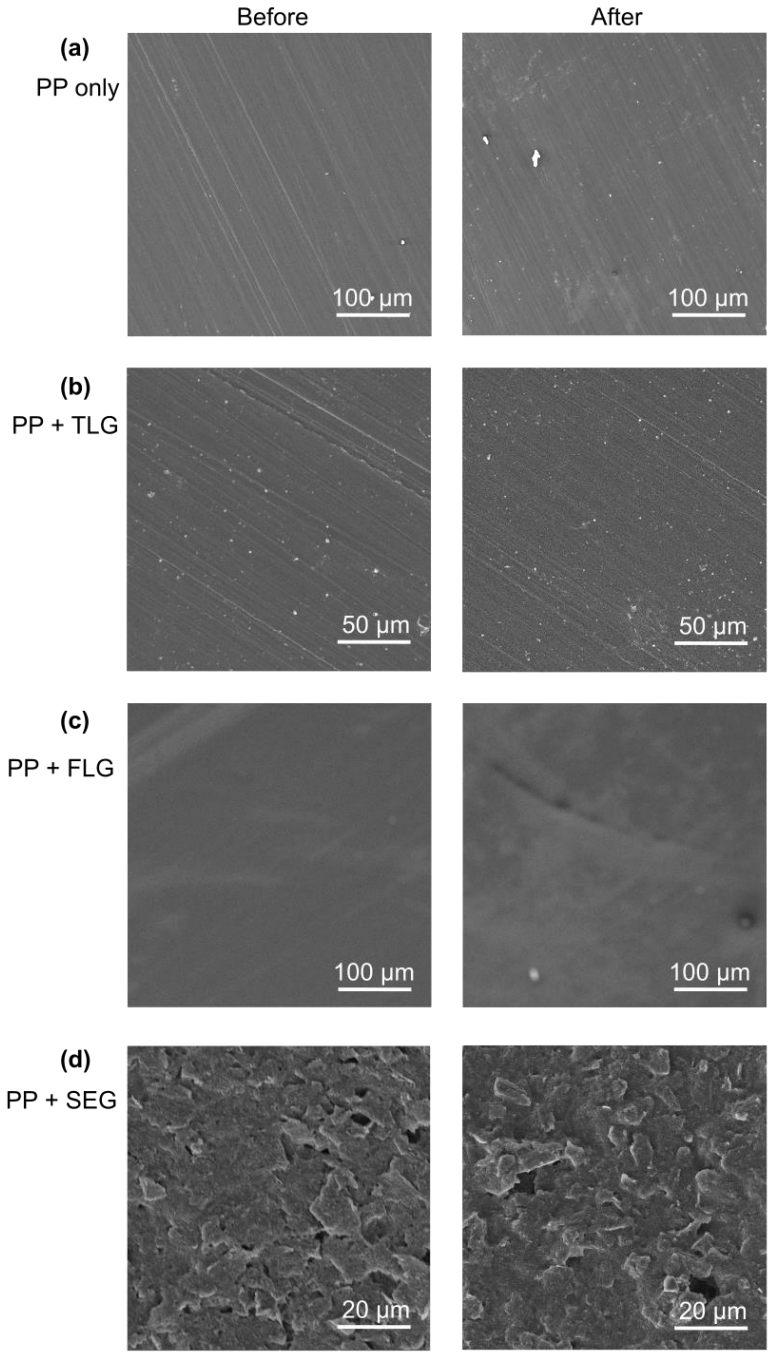

Figure S11. SEM images of: **(a)** PP fibre; and PP fibres coated with: **(b)** TLG; **(c)** FLG; and **(c)** SEG. Images on the left and right columns were taken before and after a room temperature to 70°C cycle, respectively.

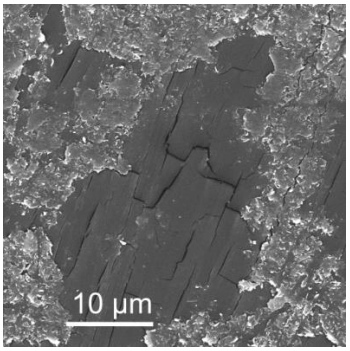

Figure S12. SEM image of a SEG coated PP fibre showing some cracks in more closely packed flakes, as well as the more lose flakes also visible in S11d.

SEG seems to provide a non-uniform coating, with several loose layers of graphene flakes over a more homogeneous film that has visible cracks (Figure S12) even before any type of manipulation that would subject the sample to mechanical or temperature stress.

5. Temperature-dependent Raman

Figure S13 shows five selected PP Raman peaks (a) and that these peaks do not shift with temperature (b).

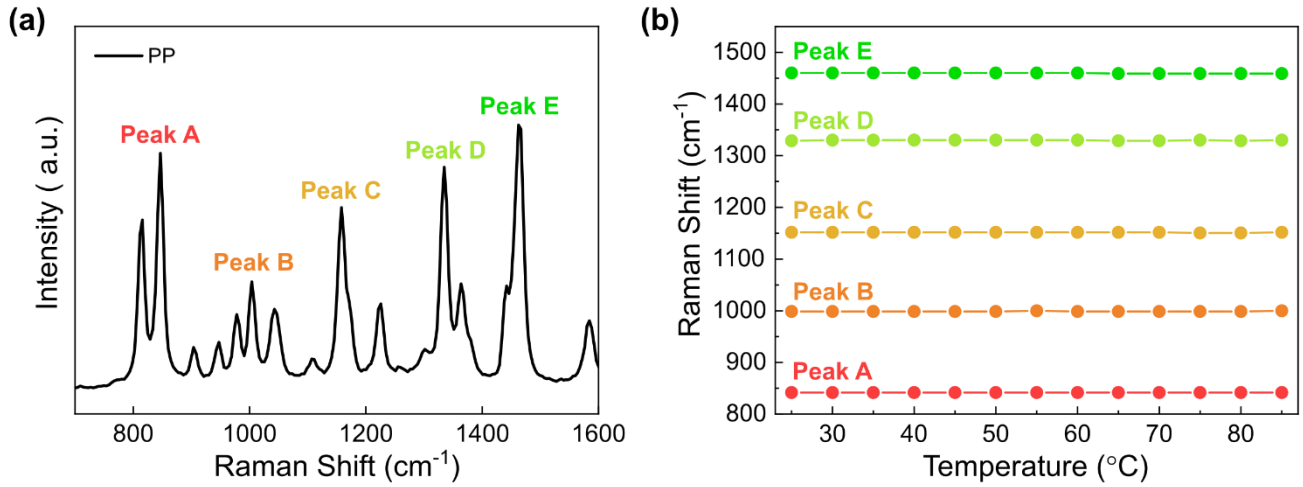

Figure S13. (a) Raman spectrum of PP highlighting the peaks studied. **(b)** Raman shift as a function of temperature for the same peaks.

6. Bending and Washability Tests

The bending test consisted of repeated bending of the fibres coated with TLG and SEG to a 5 mm radius, up to a 1000 bending cycles. As shown on the manuscript (figure 4a), the TLG sensors do not show a significant change in resistance with bending cycles. The SEG sensors are not as robust, showing degradation of performance over a large number of bending cycles. Encapsulation with a protective polymeric layer would both protect the graphene coating to make it more robust, and insulate the sensor from ambient and from the user, for a safer usage.

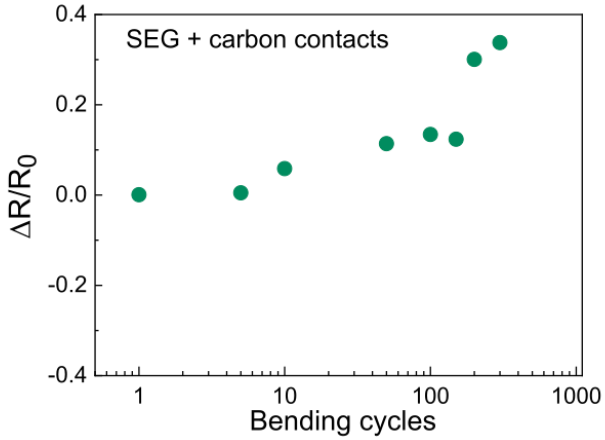

Figure S14. Sensitivity of an SEG-coated device as a function of the number of bending cycles.

Washing tests were performed by stirring the graphene coated textile fibres in a beaker with different laundry detergents and de-ionised water (DIW) using magnetic stirrer. Resistance of each sample was measured before subjecting them to washing tests. Different temperatures (30°C, 40°C and 50°C) and stirring speed (400 rpm, 800 rpm and 100 rpm) were used to emulate the washing machine. The samples were washed for 60 minutes per cycle and rinsed with DIW multiple times prior to measuring the resistance again. No encapsulation was used while performing these tests. The resistance values were normalised to the initial value (resistance at room temperature) before washing to better monitor how it changed afterwards. The detergents used were commercially available bio detergent and a non-bio detergent. A fabric softener was also used to perform the washing tests. A new CVD/SEG sample was used to perform the experiment for each of the studied stirring speeds.

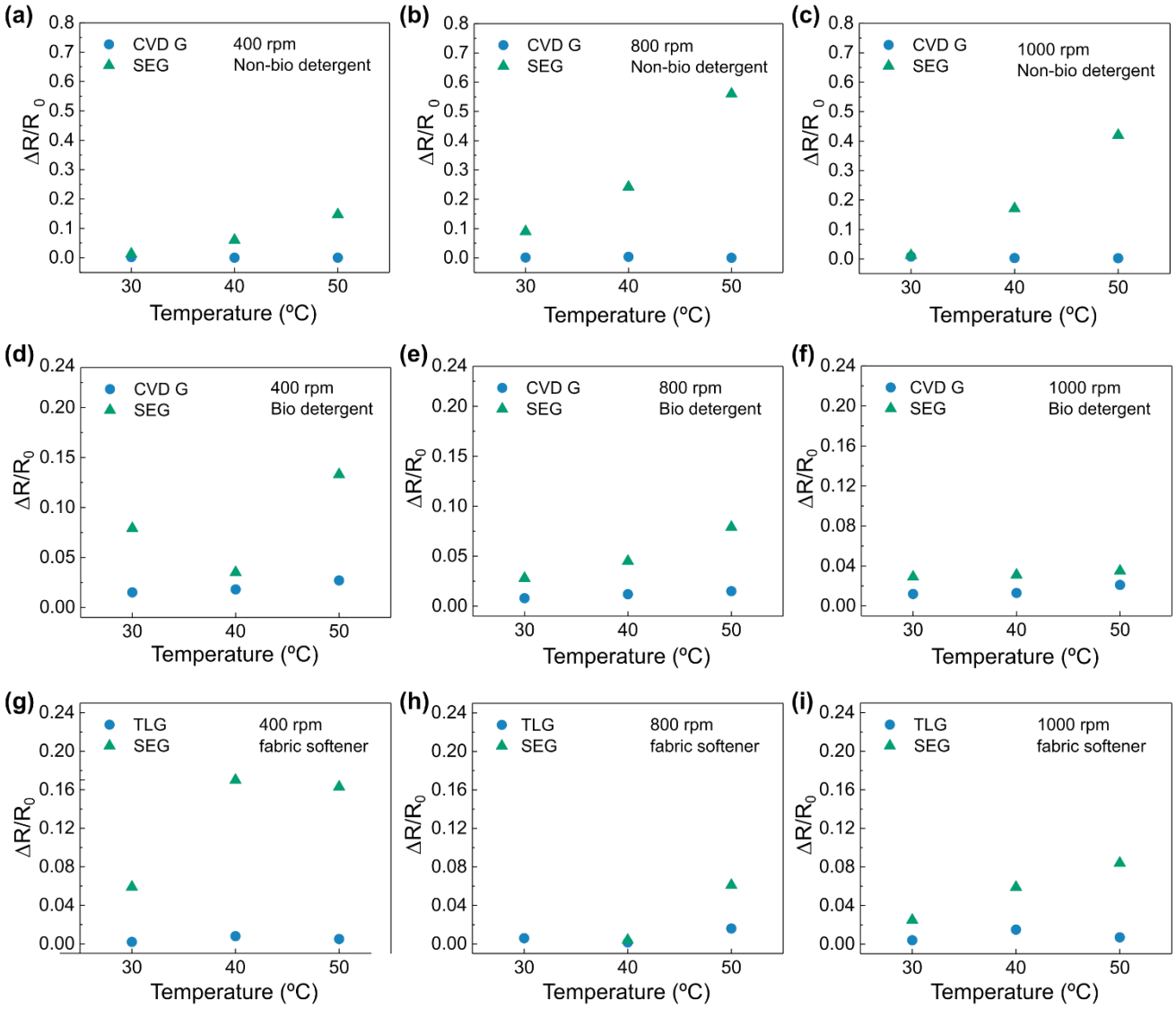

Figure S15. Normalised resistance of TLG and SLG coated PP fibres against temperature of washing test with varying rpm and different detergents: non-bio at **(a)** 400, **(b)** 800 and **(c)** 1000 rpm; bio detergent at **(d)** 400, **(e)** 800 and **(f)** 1000 rpm; and fabric softener at **(g)** 400, **(h)** 700 and **(i)** 1000 rpm.

References

[1] Zhu SE, Yuan S, Janssen GCAM 2014 Optical transmittance of multilayer graphene *EPL* **108** 17007

[2] Jhang SH *et al.* 2011 Stacking-order dependent transport properties of trilayer graphene *Phys. Rev. B* **84** 161408

[3] Pollard AJ *et al.* Good Practice Guide No. 145 - Characterisation of the Structure of Graphene. 1st ed. National Physical Laboratory, 2017.

[4] Koh YK, Bae MH, Cahill DG, Pop E 2011 Reliably Counting Atomic Planes of Few-Layer Graphene (n > 4) *ACS Nano* **5** 269